

Accuracy of the calculated unoccupied states in GaN phases as tested by high-resolution electron energy-loss spectroscopy

M. S. Moreno*

Centro Atómico Bariloche, 8400-San Carlos de Bariloche, Argentina

S. Lazar and H. W. Zandbergen

Kavli Institute of Nanoscience, Delft University of Technology, Lorentzweg 1, 2628 CJ Delft, The Netherlands

R. F. Egerton

Department of Physics, University of Alberta, Edmonton, Canada T6G 2J1

(Received 12 July 2005; published 15 February 2006)

The electronic structures of cubic and hexagonal phases of GaN have been investigated by high-resolution electron energy-loss spectroscopy in a monochromated transmission electron microscope. Both the Ga- $L_{2,3}$ and N K -edges were measured. The data are compared to the latest versions of two different calculation schemes: band structure and multiple-scattering calculations. We have found that both methods are capable of giving results that can be compared quantitatively to the experiment. Small discrepancies with experiment could be eliminated by future developments in the implementation of these methods.

DOI: 10.1103/PhysRevB.73.073308

PACS number(s): 79.20.Uv, 78.70.Dm, 82.80.Pv

The recent availability of electron-beam monochromators for high-resolution electron energy-loss spectroscopy (HREELS) in a transmission electron microscope (TEM) makes it feasible to obtain the near-edge fine structure (ELNES) of a core-loss spectrum with a precision comparable to that of x-ray absorption spectroscopy. This opportunity opens up the exciting possibility of studying the internal electronic structure of materials, combined with complete structural information (from TEM diffraction and imaging) and nanometer lateral resolution. Because ELNES is related to the angular-momentum resolved density of unoccupied states (LDOS) at the site of the excited atom,¹ high-resolution data allows us to make a comparison with state-of-the-art computer calculations. As a consequence, we should obtain greatly improved reliability of spectral interpretation. Two different *ab initio* methodologies can be compared: band structure (BS) calculations and self-consistent real-space multiple-scattering (MS) calculations. It is often assumed that the latter approach is less precise than the former because of the use of a finite cluster size; that it is convenient for obtaining fast results but that its usefulness is limited to qualitative comparisons. However, both approaches (in their latest developments) allow inclusion of the effects of the core-hole left by the excited electron, using approximations that are an improvement on the $Z+1$ approximation previously used in such calculations.^{2,3}

GaN and its alloys have attracted much research in recent years due to their applications.^{4,5} At present, GaN nanowires are receiving particular attention since they have possible application as high-mobility field-effect transistors and miniaturized UV-blue nanolasers. Recent work has stressed the importance of sub-band-gap states in this material in relation to potential applications.⁶⁻⁹ States close to the Fermi energy relate directly to the scattering and recombination mechanisms that determine the concentration of carriers. Thus the use of bulk or nanostructured material requires, as a prereq-

uisite to understanding more complex problems, a precise knowledge of the density of unoccupied states. Although there have been previous calculations for GaN, using BS¹⁰⁻¹³ and/or MS calculations,^{14,15} they involved qualitative comparisons to data of limited resolution. In this work we present a complete set of ELNES measurements for the cubic and hexagonal phases of GaN, obtained by monochromator-assisted EELS. We make quantitative comparison of these experimental results with ELNES calculated using the BS and MS methods. The influence of the angular dependence is also analyzed.

Hexagonal and cubic samples were grown by metal-organic chemical-vapor deposition on a sapphire substrate and a 3C-SiC substrate, respectively, as described in Ref. 10. For the HREELS experiments, we used an FEI Tecnai 200FEG equipped with a prespecimen monochromator and a high-resolution imaging filter.¹⁶ Using an accelerating voltage of 200 kV, the energy resolution [measured as the full width at half maximum (FWHM) of the zero-loss peak] was 0.2 eV for the N-edge and 0.55 eV for the Ga $L_{2,3}$ edge. The difference in energy resolution of the two edges comes from the fact that the N K -edge was acquired with the monochromator ON and the Ga $L_{2,3}$ edges with the monochromator switched OFF, as required to obtain adequate intensity and good signal-to-noise ratio. The fact the monochromator was OFF does not affect the quality of these measurements because the intrinsic width of the Ga $L_{2,3}$ edges is higher (0.76 eV) than the energy resolution of the experiment (0.55 eV). The spectra were recorded in TEM diffraction mode from thin regions of the sample ($t/\lambda < 0.4$, λ being the inelastic mean free path of the electrons) and corrected for dark current and channel-to-channel gain variation of the charge coupled device detector. The preedge background was subtracted according to a power-law model.

MS calculations were performed using the FEF8.20 code¹⁷ using Hedin-Lundqvist self-energies (i.e., complex

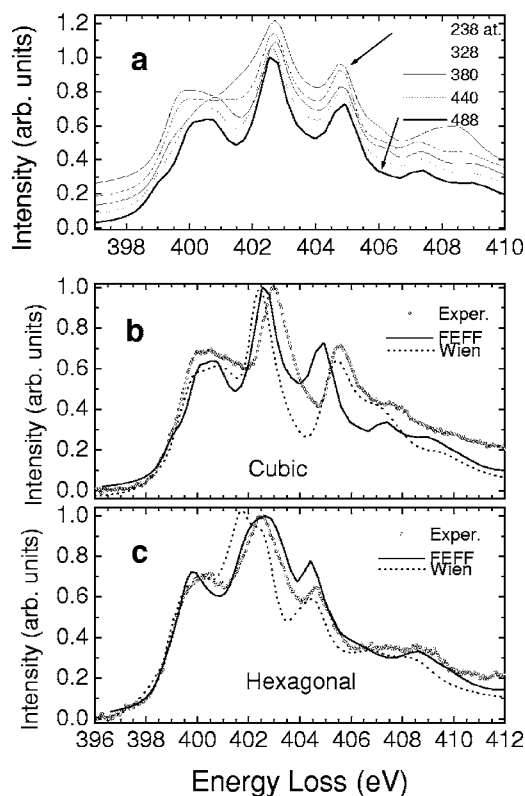


FIG. 1. Experimental and calculated N K -edge for both phases. In the upper panel is shown the dependence of the calculated spectrum for the cubic phase as a function of the cluster size used for the full MS scattering calculation. The hexagonal spectrum corresponds to the averaged case.

exchange-correlation potentials) to account for inelastic losses. In the construction of the muffin-tin potentials, we allowed for different degrees of overlapping of the muffin tins in order to reduce discontinuity effects at the muffin-tin edges and to roughly determine the need for nonspherical corrections to the potentials. In contrast with previous reports for this material,^{14,15} we have found that relatively large cluster sizes are needed, first to get well-converged potentials (about 100 atoms) and then to ensure precise full-MS calculations (about 480–500 atoms); see Fig. 1. We considered the influence of final-state effects resulting from the core-level excitation. The core-hole effect was approximated using the *final state rule*: the potential of the final states includes a fully screened core hole which is calculated self-consistently. We concluded that the experimental spectrum is better reproduced by including this core-hole effect in the calculation of the edges of both phases. Finally, broadening was added to account for the experimental energy resolution.

The BS calculations were done using the Wien2k program.¹⁸ The core-hole effect is taken into account by changing the occupancy of the core electron involved in the excitation process, the missing charge being added as a uniform background. The program allows us to consider partial core holes (i.e., fractional occupancies of the core level).³ In order to account for the core-hole effect, a supercell is needed to avoid the interaction between neighboring core holes. The ELNES were calculated using the TELNES pro-

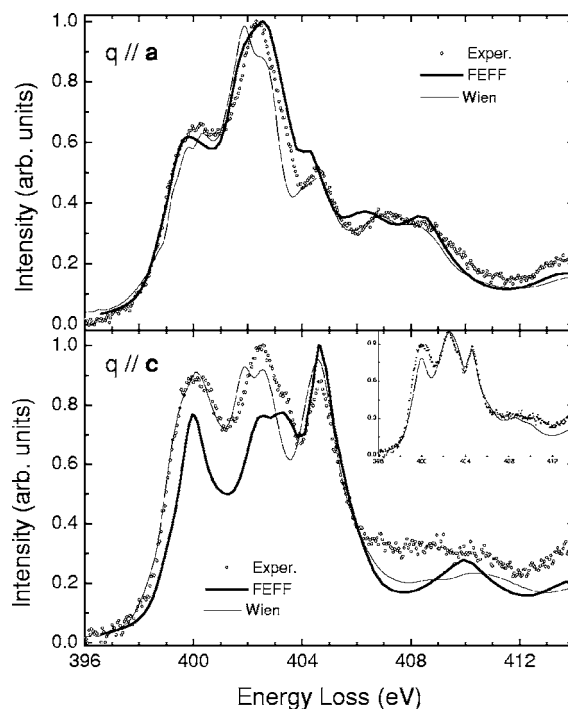


FIG. 2. Experimental and calculated spectra for the N K -edge of the hexagonal phase for two different main directions for the momentum transfer \mathbf{q} . Spectra for transitions to (upper) p_{xy} and (lower) p_z final states are plotted. Collection semiangle was 0.4 mrad. In the inset the data are compared to a linear combination of the two MS calculations.

gram (in the Wien2k distribution) according to the formalism of Ref. 19. This program allows us to take into account the orientation and anisotropy of the specimen and integrates the spectrum over the experimental collection and convergence angles. The N K -edge in the hexagonal polytype was calculated exploiting all these capabilities of the software. We experimented with supercells of different sizes, the final calculations employing a $2 \times 2 \times 2$ supercell (32 atoms). The best match was obtained for 0.55 core-hole occupancy for the N K -edge and a full core hole for the Ga $L_{2,3}$ edges for both polytypes.²⁰ To incorporate the experimental energy resolution, the calculated spectra were convolved with a Gaussian function of 0.2 eV FWHM for the N K -edge and 0.55 eV FWHM for the Ga $L_{2,3}$ edges. Excited-state lifetime broadening was taken into account by broadening the simulated spectrum with a Lorentzian of width $=0.1E$, where E is the energy above Fermi level.²¹ A Lorentzian of 0.1 eV FWHM for the N K -edge and 0.76 eV for Ga $L_{2,3}$ edges has been used to account for broadening due to the core-hole lifetime.²² To ensure good convergence, major parameters such as the number of k points in the Brillouin zone and $Rmt \cdot Kmax$ (where Rmt is the smallest atomic radii and $Kmax$ is the cutoff in the plane wave expansion of wave functions) have been chosen such that any increases of the values does not significantly affect the ELNES. Final values used were $Rmt \cdot Kmax = 7500$ k -points for the hexagonal case and 400 k -points for cubic crystals.

In Figs. 1–3 we show the experimental N- K and Ga- L_3 edge for both phases, together with our results using both the

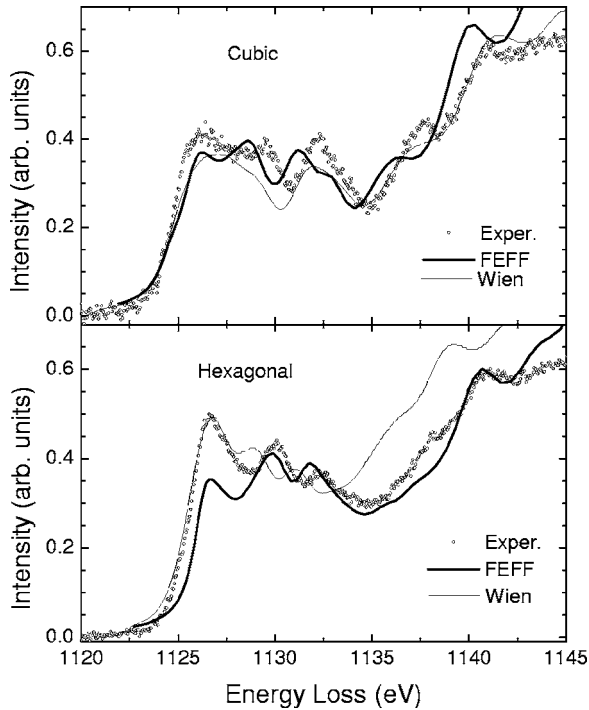


FIG. 3. Experimental and calculated Ga L_3 -edge for cubic and hexagonal phases. Collection semiangle was 6 mrad.

MS and BS methods. In general, both approaches reproduce the energy scale and intensity dependence with similar precision. For the MS method we can see, for both edges, the same behavior: for the hexagonal phase this method reproduces the energy scale with high precision, while for the cubic phase this method shows a small but progressive (with energy) mismatch with experiment. These differences in the predicted energy scale may reflect either the need of using an even bigger cluster size for the cubic phase (see next paragraph) or a different degree of suitability of the self-energy model, perhaps due to differences in the electronic properties of both phases. The BS method yields highly acceptable results, considering that it is not intended for the calculation of excited states.

Figure 1(a) shows the spectrum for the cubic phase and its dependence on the cluster size used for the MS calculation. The choice of the cluster size mainly affects the near edge region but also the structure seen at 407–410 eV. The evolution of the latter region reveals that the correct number of peaks in the spectrum are obtained by using a cluster of at least 328 atoms. For even bigger clusters, the near-edge region is most sensitive to cluster size. Another effect of convergence is a progressive separation between the first peak and subsequent peaks. The calculated spectrum reaches a satisfactory convergence for a cluster size of around 490 atoms. For hexagonal GaN we found that big clusters, of about 480 atoms, are also needed to get the better matching to HREELS data. These values are larger than those used in previous calculations [50 (Ref. 15) or 120 atoms¹⁴], suggesting that these earlier calculations were not fully converged. In both cases small discrepancies with experiment can only be appreciated by comparison with high-resolution spectra, like the present ones. Otherwise, they can go unnoticed. In

Figs. 1(b) and 1(c), we present our results for the cubic and hexagonal phase. It has been shown by calculating the p_{xy} and p_z partial DOS that the first and third peaks are dominated by N p_z states and the second and fourth peaks by p_{xy} states,^{10,13} in agreement with the spectra shown in Fig. 2. Structures (not shown) occur in the Ga and N partial DOS at the same energies, a good indication that hybridization must play an important role in these materials. The N DOS has a $2p$ character in the energy range studied here. The first peak in the Ga DOS contains almost equal contributions from s , p , and d states, while s states predominate in the second. The other two peaks are mainly due to Ga p states.

For the hexagonal phase we note that the BS result reproduces well the spectrum shape close to the edge, where the MS calculation fails to give the right profile, perhaps because hybridization effects are not fully taken into account. Because of its noncentrosymmetric unit cell, the hexagonal phase is anisotropic, an aspect that must be considered for both experiment and calculations. The calculated spectra presented in Fig. 1(b) correspond to a spherical average over all orientations of the momentum-transfer vector. These spectra should properly be compared to experimental data acquired with a collection semiangle β equal to the so-called magic angle, such that the structure is independent of specimen orientation. A fully relativistic estimate gives $\beta=1.5$ mrad²³ or 1.7 mrad²⁴ for the N K -edge, whereas the experimental spectrum shown in Fig. 1(c) was acquired at $\beta=1.9\pm 0.2$ mrad. Thus the small difference in the intensity of the peak at 404.6 eV might be due to this discrepancy. Because of the anisotropy of the hexagonal phase, the intensity of this peak is strongly sensitive to the sample orientation and to the collection semiangle, as we see from Fig. 2.

Experimentally, we can study anisotropies in the electronic structure by selecting a momentum transfer vector (\mathbf{q}) parallel or perpendicular to the \mathbf{c} axis, such that transitions (from the N $1s$ state) to the p_z or p_{xy} -symmetry-projected states are probed. Because of the size of the apertures used to form the probe and collect the scattering, we actually have a range of incident and collection angles. The momentum-transfer direction can be selected by adopting the corresponding collection condition.²⁵ In Fig. 2, we show spectra corresponding mainly to momentum transfer perpendicular ($\mathbf{q}\perp\mathbf{c}$) and parallel ($\mathbf{q}\parallel\mathbf{c}$) to the \mathbf{c} axis. The case $\mathbf{q}\perp\mathbf{c}$ corresponds to transitions to states of symmetry p_{xy} which should dominate the spectrum for a collection semiangle higher than the magic angle, for an incident beam along the \mathbf{c} direction. This is so because there are three p_{xy} orbitals for each p_z orbital. Consequently, the spectrum is less affected by the choice of β mentioned. This choice is more important for the case $\mathbf{q}\parallel\mathbf{c}$. For our experimental conditions, we have estimated the perpendicular contribution to be about 40%. This contribution explains the almost flat region between 406 and 411 eV in the spectrum. Because the finite collection semiangle is not taken into account in the MS calculations, we attribute the discrepancy in the peak intensity to this effect. The BS calculation allows inclusion of this spread and gives a better agreement with the experiment. In this sense, our MS calculation corresponds to the ideal situation of $\beta=0$, when only one direction in the specimen (parallel or perpendicular to the \mathbf{c} axis) is excited. When both contribu-

tions are combined, it is possible to greatly improve the intensity for the $\mathbf{q} \parallel \mathbf{c}$ case (shown in the inset of the Fig. 2), the agreement being equivalent to that obtained from the BS calculations. Here we have presented the ideal cases because they serve as a guide to understanding how a real spectrum ($\beta \neq 0$) is built from the two momentum components.

In Fig. 3 we show the Ga L_3 -edge for both phases. This edge arises from transitions of p states to s and d states. The results of the MS method (not shown) indicate that the first transition contributes with approximately 25% of the total intensity to the first and second peaks. The BS calculations suggest a less important contribution of this transition (approximately 20%) and that it only reinforces the first peak of the Ga L_3 spectrum.¹⁰ For this edge, the influence of the core hole is less important, although its inclusion in the calculations provides slightly better matching to the experimental data. For cubic GaN, the MS calculation reproduces the intensity satisfactorily. For the hexagonal phase, the BS calculation gives better matching of the experimental intensity near the threshold. We also note that the MS calculation gives a slightly lower intensity in the near-edge region for both phases, in contrast to the good matching for the N edge

obtained, presumably reflecting the approximations made in the calculations, such as the spherical potential; nonspherical effects can affect the relative heights of the near-edge peaks.²⁶

In summary, we have compared BS and MS calculations to high-resolution EELS data of cubic and hexagonal GaN. For the hexagonal phase, we also examined contributions from transitions along directions parallel and perpendicular to the c axis. In the case of MS calculations we demonstrated the importance of having a large enough cluster size in order to obtain a good match with high resolution data. This was not necessary for comparison with “normal” data because the fine structure and the contribution from high-order neighboring shells were simply not visible due to the poor resolution. Provided care is taken to ensure good convergence, we find that both methods are capable of giving quantitative agreement with experimental data. Better agreement with experiment may require further developments in the implementation of these two methods.

M.S.M. thanks the partial financial support of CONICET, Argentina.

*Electronic address: smoreno@cab.cnea.gov.ar; Also at CONICET.

¹R. F. Egerton, *Electron Energy-Loss Spectroscopy in the Electron Microscope* (Plenum, New York, 1996).

²J. J. Rehr and R. C. Albers, *Rev. Mod. Phys.* **72**, 621 (2000).

³C. Hbert, Joachim Luitz, and P. Schattschneider, *Micron* **34**, 219 (2003).

⁴S. Nakamura, T. Mukai, and M. Senoh, *Appl. Phys. Lett.* **64**, 1687 (1994).

⁵S. Nakamura, N. Iwasa, M. Senoh, S. Nagahama, T. Yamada, and T. Mukai, *Jpn. J. Appl. Phys., Part 2* **34**, L1332 (1995).

⁶Z. Liu, F. Machuca, P. Pianetta, W. E. Spicer, and R. F. W. Pease, *Appl. Phys. Lett.* **85**, 1541 (2004).

⁷P. W. Yu, J. D. Clark, D. C. Look, C. Q. Chen, J. Yang, E. Koutstis, M. A. Khan, D. V. Tsvetkov, and V. A. Dmitriev, *Appl. Phys. Lett.* **85**, 1931 (2004).

⁸A. Shabaev and Al. L. Efros, *Nano Lett.* **4**, 1821 (2004).

⁹I. Arslan, A. Bleloch, E. A. Stach, and N. D. Browning, *Phys. Rev. Lett.* **94**, 025504 (2005).

¹⁰S. Lazar, C. Hébert, and H. W. Zandbergen, *Ultramicroscopy* **98**, 249 (2004).

¹¹S. P. Gao, A. Zhang, J. Zhu, and J. Yuan, *Appl. Phys. Lett.* **84**, 2784 (2004).

¹²T. Mizoguchi, I. Tanaka, S. Yoshioka, M. Kunisu, T. Yamamoto, and W. Y. Ching, *Phys. Rev. B* **70**, 045103 (2004).

¹³V. J. Keast, A. J. Scott, M. J. Kappers, C. T. Foxon, and C. J. Humphreys, *Phys. Rev. B* **66**, 125319 (2002).

¹⁴I. Arslan and N. D. Browning, *Phys. Rev. B* **65**, 075310 (2002).

¹⁵T. Chassé, K. H. Hallmeier, J.-D. Hecht, and F. Frost, *Surf. Rev. Lett.* **9**, 381 (2002).

¹⁶S. Lazar, G. A. Botton, M.-Y. Wu, F. D. Tichelaar, and H. W. Zandbergen, *Ultramicroscopy* **96**, 535 (2003).

¹⁷A. L. Ankudinov, B. Ravel, J. J. Rehr, and S. D. Conradson, *Phys. Rev. B* **58**, 7565 (1998).

¹⁸P. Blaha, K. Schwarz, G. Madsen, D. Kvasnicka, and J. Luitz, *WIEN 2k, An Augmented Plane Wave+Local Orbital Program for Calculating Crystal Properties* (Karlheinz Schwarz, Techn. Universitt Wien, Austria, 2001).

¹⁹M. Nelhiebel, P. H. Louf, P. Schattschneider, P. Blaha, K. Schwarz, and B. Jouffrey, *Phys. Rev. B* **59**, 12807 (1999).

²⁰S. Lazar, C. Hébert, and H. W. Zandbergen, *Microsc. Microanal.* **10** (Suppl. 2), 884 (2004).

²¹C. Hébert, M. Kostner, and P. Schattschneider, *Proceedings of the EUREM-XII, Brno, Czech Republic, 2000, Vol. 3*, pp. 333–334.

²²*Unoccupied Electronic States*, edited by J. C. Fuggle and J. E. Inglesfield (Springer, Berlin, 1992).

²³B. Jouffrey, P. Schattschneider, and C. Hébert, *Ultramicroscopy* **102**, 61 (2004).

²⁴Y. K. Sun and J. Yuan (private communication).

²⁵R. D. Leapman and J. Silcox, *Ultramicroscopy* **9**, 349 (1979).

²⁶H. Modrow, S. Bucher, J. J. Rehr, and A. L. Ankudinov, *Phys. Rev. B* **67**, 035123 (2003).